Juni Khyat
(UGC Care Group I Listed Journal)
ISSN: 2278-4632
Vol-10 Issue-3 No.01 March 2020

Impedance-Based Local Stability Criterion for DCDistributed Power Systems

[1*] Ms.Ekata Kanungo, [2] Mr.Bikash Kumar Swain

[1*] *Asst. Professor, Dept. Of Electrical Engineering, NIT BBSR,*
Asst. Professor DEPT. of Electrical Engineering, NIT BBSR,
[1]ekata@thenalanda.com*, , bikashkumar@thenalanda.com

***Abstract*—This paper addresses the stability issue of dc dis- tributed power systems (DPS). Impedance-based methods are effective for stability assessment of voltage-source systems and current-source systems. However, these methods may not be suit- able for applications involving variation of practical parameters, loading conditions, system's structures, and operating modes. Thus, for systems that do not resemble simple voltage-source systems or current-source systems, stability assessment is much less readily performed. This paper proposes an impedance-based criterion for stability assessment of dc DPS. We first classify any converter in a dc DPS as either a bus voltage controlled converter (BVCC) or a bus current controlled converter (BCCC). As a result, a dc DPS can be represented in a general form regardless of its structure and operating mode. Then, the minor loop gain of the standard dc DPS is derived precisely using a two-port small signal model. Application of the Nyquist criterion on the derived minor loop gain gives the stability requirement for the dc DPS. This proposed criterion is applicable to dc DPSs, regardless of the control method and the connection configuration. Finally, a 480 W photovoltaic (PV) system with battery energy storage and a 200 W dc DPS, in which the source converter employs a droop control, are fabricated to validate the effectiveness of the proposed criterion.**

***Index Terms*—Battery energy storage, DC distributed power system (DPS), photovoltaic system, stability criterion.**

I. INTRODUCTION

THE DC distributed power system (DPS) has been widely used in application environments such as space stations, aircraft, shipboards, hybrid vehicles, communication systems, and renewable energy systems, thanks to its flexible system con- figuration, high efficiency, and high power-density delivery ca-pability [1]–[7]. However, the dc DPS may become unstable due to interaction between the subsystems, even though each sub-system may operate properly as an individual system [8]–[14]. The impedance-based method has been effective for as- sessing stability and its use has been rapidly growing for various dc DPS applications ranging from conventional interconnected dc/dc systems to grid-connected renewable energy systems. The foundation of the impedance-based stability and transient

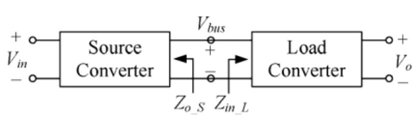

Fig. 1. Cascaded system.

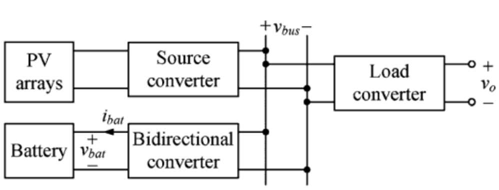

Fig. 2. Standalone PV-battery hybrid power system.

performance analysis was laid down in 1976 by Middlebrook who proposed a set of input-filter design rules for regulated converters [15]. It was shown that, for the typical cascaded system shown in Fig. 1, the ratio of the source converter's output impedance and load converter's input impedance Z_{in_L}, Z_{o_S} , can be equivalently represented in terms of Z_{o_S}/Z_{in_L} the loop gain of the cascaded system. It was also pointed out that, if both the source converter and the load converter are stable individually, and Z_{o_S} is less than Z_{in_L} in the entire frequency range, the stability of the cascaded system will be guaranteed. This is the so-called *Middlebrook criterion*. Subsequently, var- ious impedance criteria aiming at more accurate and practical assessment of stability associated with subsystems' interaction have been developed during the past three decades [16]–[20]. Recently, it has been found that the impedance ratio has to be selected in a certain way for assessing correctly the stability in the voltage-source system and the current-source system [21], i.e., if the source converter is controlled as a voltage source, the impedance ratio should be Z_{o_S}/Z_{in_L}, whereas if the source converter is controlled as a current source, the impedance ratio will be Z_{in_L}/Z_{o_S}.

However, not all dc DPSs can be treated simply as a voltage-source system or current-source system. Thus, the existing impedance-based stability criteria may not be adequate in some special applications. For instance, the typical stand- alone photovoltaic-battery hybrid power system, as shown in Fig. 2 [22], is a system which is far more complex than a voltage-source system or current-source system. It contains photovoltaic (PV) arrays, a source converter, a load converter and a bidirectional dc/dc converter and battery. In this system, the source converter delivers energy from the PV arrays to the dc bus. The load converter converts the energy from the dc bus to the system's load. Meanwhile, the battery makes up the difference between the source and the load via the bidirectional converter. According to the amount of power supplied by the PV arrays, which depends on the sunlight intensity and temperature, as well as the state of charge (SOC) of the battery, the standalone PV-battery hybrid power system has five pos- sible operating modes, as shown in Table I and Fig. 3. In the following description, and P_o denote the output power of

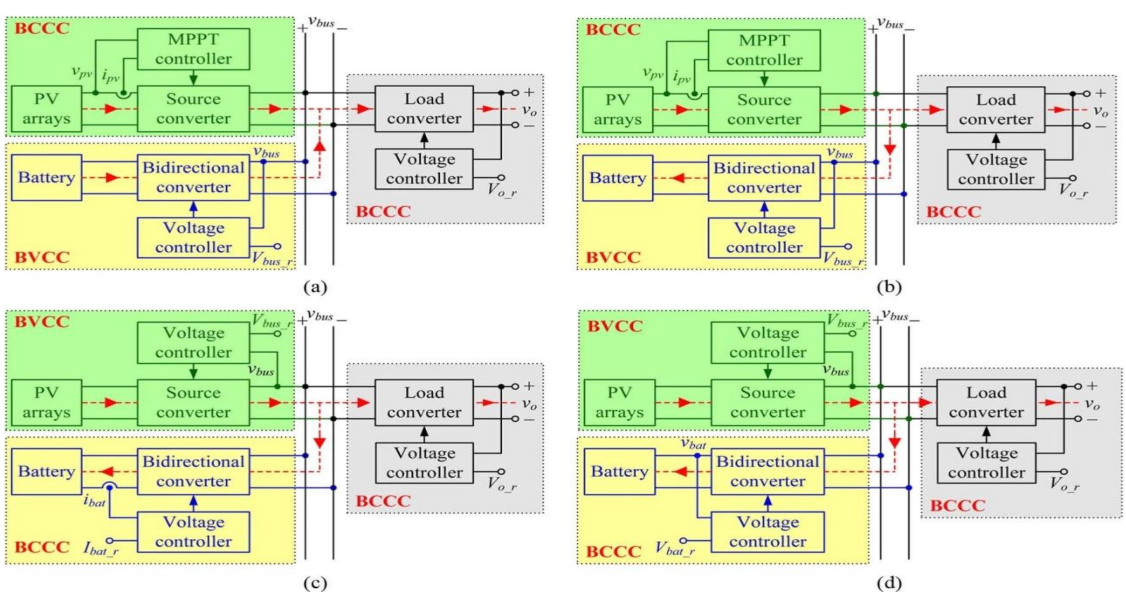

Fig. 3. Power flow schematics of standalone PV-battery hybrid power system in operating modes: (a) II, (b) III, (c) IV, and (d) V.

ISSN: 2278-4632
Vol-10 Issue-3 No.01 March 2020

TABLE I
OPERATING MODES AND CONDITIONS FOR THE STANDALONE PV POWER SYSTEM

	$P_{pv}<P_o$	$P_{pv}\geq P_o$, $i_{bat}<I_{bmax}$	$P_{pv}\geq P_o$, $i_{bat}\geq I_{bmax}$
$v_{bat}\leq V_{bmin}$	Mode I	Mode III	Mode IV
$V_{bmin}<v_{bat}<V_{bmax}$	Mode II	Mode III	Mode IV
$v_{bat}\geq V_{bmax}$	Mode II	Mode V	Mode V

the PV arrays and load converter, respectively. Also, V_{bmin} and V_{bmax} denote the permitted minimum and maximum battery voltages, respectively, and I_{bmax} denotes the charge current limit.

Operating Mode I: If $P_{pv} < P_o$ and the battery is deeply discharged, the whole system is shut down. In this mode, the system does not suffer an instability problem.

Operating Mode II [Fig. 3(a)]: If $P_{pv} < P_o$ and the battery is able to provide power, the PV arrays feed as much power aspossible to the load with the maximum power point tracking (MPPT) algorithm enabled. At the same time, the battery pro-vides complementary power through the bidirectional converter by regulating the bus voltage v_{bus}. In this mode, both the sourceconverter and bidirectional converter are source converters, and they are controlled as power source and voltage source, respec-tively. Therefore, the standalone PV-battery hybrid system with mode II cannot be treated simply as a voltage-source systemor current-source system. In other words, the existing criteriacannot be used to analyze system's stability directly in this case. *Operating Mode III* [Fig. 3(b)]: If $P_{pv} > P_o$ by a small margin and the battery is not in full state, then the excess solarpower is used to charge the battery. In this mode, the source con- verter is also controlled as a power source instead of a voltage or current source. Therefore, the existing stability criteria are not applicable in this mode as well.

Operating Mode IV [Fig. 3(c)]: If $P_{pv} > P_o$ by a large margin and the PV arrays can simultaneously power the load and charge the battery with constant current I_{bmax}. Here, the bidirectional converter controls the charging current of battery, and the source converter will regulate v_{bus} with MPPT controller disabled. In this mode, the standalone PV-battery hybrid system is a voltage-source system, and the Middlebrook criterion can be applied to assess the stability of the system.

Operating Mode V [Fig. 3(d)]: If $P_{pv} > P_o$ and the battery is fully charged, the charge method is switched to constant voltage charging (floating charging) to prevent self-discharge of the bat- tery. In this situation, the system is also a voltage-source system, and its stability can also be determined by the Middlebrook cri-terion.

As described above, the standalone PV-battery hybrid system switches its operating mode from time to time. In modes II and III, the system does not behave as a voltage-source system or current-source system. As a result, assessing the system's sta- bility becomes non-trivial.

Our first aim in this paper is to find a concise criterion to as- sess the stability of the above complex dc DPS. The second aim is to extend the proposed criterion to more general dc DPS appli- cations, including the voltage-source system, the current-source system, the dc DPS whose source converter utilizes the droop control, and the dc DPS with series-parallel connected system. Section II describes a crucial preparatory step to arriving at a stability criterion, which involves treating converters in the dc DPS as either a bus voltage controlled converter (BVCC) or a bus current controlled converter

(BCCC), rather than the traditional source and load con- verters. As a result, the dc DPS can be

.

described by a standard form regardless of its structure and operating mode. Section III presents the derivation of the proposed criterion. A minor loop gain of the standard dc DPS is derived using a two-port small signal model and the impedance-based stability criterion is proposed. Section IV extends the proposed criterion to general dc DPS applications, and reveals the relationship between the proposed criterion and the existing criteria. In Section V, a 480 W standalone PV-battery hybrid system and a 200 W dc DPS, whose source converters employ a droop control strategy,

are constructed. The effectiveness of the proposed impedance criterion is verified experimentally.

II. DESCRIPTION OF DC DISTRIBUTED POWER SYSTEM

As mentioned earlier, the biggest challenge in stability anal- ysis of the complex dc DPS is the changing operating mode, and in some operating modes, the system cannot be treated as a conventional voltage-source system or current-source system. In this section, we consider the dc DPS from a new perspective and describe it by a standard form which does not depend on the specific operating mode.

A. Concepts of Bus Voltage Controlled and Bus Current Controlled Converters

In a dc DPS, there are one or more dc buses connecting the system's converters. For a dc bus, there are two variables, namely, the bus voltage and the bus current. Hence, we may classify a dc DPS converter into two basic types according to the bus variable being controlled. Specifically, any converter in a dc DPS is either a bus voltage controlled converter (BVCC) or a bus current controlled converter (BCCC):

1) BVCC refers to a converter that controls or affects its *bus-side-port-voltage*.
2) BCCC refers to a converter that controls or affects its *bus-side-port-current*.

In order to explain the concepts of BVCC and BCCC clearly, we take the standalone PV-battery hybrid system as an example, which has been shown in Fig. 3.

In operating mode I, the whole system is shut down. There- fore, it is meaningless to classify a converter as BVCC or BCCC for this operating mode.

In operating mode II, the bus voltage is controlled by the bidi- rectional converter directly, and the bidirectional converter is therefore BVCC. Since the bus voltage is already regulated by the bidirectional converter, the source converter and load con- verter can only affect the bus current by regulating their power, i.e., the source converter controls its bus-side-port-current by regulating its input power using a MPPT technique. In this case, the load converter changes its bus-side-port-current by changing the load condition. Therefore, both the source converter and load converter are BCCCs, as shown in Fig. 3(a).

Likewise, in operating mode III, the bidirectional converter is BVCC, and both the source converter and the load converter are BCCCs, as shown in Fig. 3(b).

In operating mode IV, the bus voltage is controlled by the source converter directly, and the source converter is BVCC. Since the bus voltage has already been controlled by the source converter, the bidirectional converter and the load converter can only affect the bus current by regulating their power, i.e., the bidirectional converter affects its bus-side-port-current by changing the reference of the battery's charging current whereas the load converter affects its bus-side-port-current by regulating its output power. Hence, both the bidirectional converter and load converter are BCCCs, as shown in Fig. 3(c).

Likewise, in operating mode V, the source converter is BVCC, and both the bidirectional converter and the load con- verter are BCCCs, as shown in Fig. 3(d).

B. Description of the DC DPS

ISSN: 2278-4632
Vol-10 Issue-3 No.01 March 2020

Based on BVCC and BCCC, we can readily put any dc DPS in a standard form. As shown in Fig. 4, in the standard form, $m\ (m \quad 1)$ BVCCs and $(n \quad 1)$ BCCCs are connected to the same dc bus in parallel. Each BVCC controls or affects its

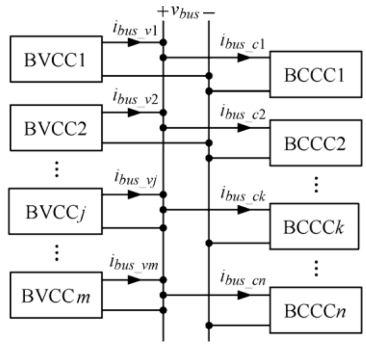

Fig. 4. General form of dc DPS.

own bus-side-port-voltage individually, and each BCCC con-trols or affects its own bus-side-port-current individually. Here, $i_{bus\_vj}\ (j = 1, 2, \ldots, m)$ and $i_{bus\_ck}\ (k = 1, 2, \ldots, n)$ are the bus-side-port-current of the jth BVCC and the kth BCCC, re-spectively.

III. STABILITY CRITERION AND MINOR LOOP GAIN OF VARIABLE STRUCTURE DC DPS

From the foregoing analysis, any dc DPS can be put in a stan- dard form, as shown in Fig. 4, regardless of the operating mode. Using this standard form, the minor loop gain of any dc DPS can be derived using a two-port small-signal model [23].

First, as shown in Fig. 5, the standard form of dc DPS con- sists of a small-signal two-port model, where all BVCCs and BCCCs are modeled as two-port networks with four input-to-output transfer functions. The definitions of the variables and input-to-output transfer functions of the two-port networks cor- responding to BVCCs and BCCCs are described in Table II. In addition, in Fig. 5, i_{bus} is the sum of all the bus-side-port-cur- rents of the BCCCs. Moreover, it can be decomposed into dif- ferent bus-side-port-currents of BVCCs, as shown in the bottom of the Fig. 5.

Then, according to Fig. 5, the input variables of the dc DPS are $\hat{X}_{vj}$ and $\hat{X}_{ck}$, and the output variables of the dc DPS are $\hat{Y}_{vj}$ and $\hat{Y}_{ck}$. Therefore, there are six input-to-output transfer functions of the dc DPS, i.e.,

$$\left.\frac{\hat{y}_{vj}}{\hat{x}_{vj}}\right|_{\hat{x}_{vj'}=0,\hat{x}_{ck}=0},\quad \left.\frac{\hat{y}_{vj'}}{\hat{x}_{vj}}\right|_{\hat{x}_{vj'}=0,\hat{x}_{ck}=0},\quad \left.\frac{\hat{y}_{ck}}{\hat{x}_{vj}}\right|_{\hat{x}_{vj'}=0,\hat{x}_{ck}=0},$$
$$\left.\frac{\hat{y}_{ck}}{\hat{x}_{ck}}\right|_{\hat{x}_{vj}=0,\hat{x}_{ck'}=0},\quad \left.\frac{\hat{y}_{ck'}}{\hat{x}_{ck}}\right|_{\hat{x}_{vj}=0,\hat{x}_{ck'}=0} \text{ and } \left.\frac{\hat{y}_{vj}}{\hat{x}_{ck}}\right|_{\hat{x}_{vj}=0,\hat{x}_{ck'}=0},$$

where $j' = 1, 2, \ldots m, j' \neq j, k' = 1, 2, \ldots, n, k' \neq k$. These transfer functions are given as follows:

$$\left.\frac{\hat{y}_{vj}}{\hat{x}_{vj}}\right|_{\hat{x}_{vj'}=0,\hat{x}_{ck}=0} = G_{BVCCj\_1} + \frac{G_{BVCCj\_2}G_{BVCCj\_3}}{Z_{v\_busj}} - \frac{G_{BVCCj\_2}G_{BVCCj\_3}Z_{v\_bus}}{Z_{v\_busj}^2 \cdot (1+T_m)} \tag{1}$$

$$\left.\frac{\hat{y}_{vj'}}{\hat{x}_{vj}}\right|_{\hat{x}_{vj'}=0,\hat{x}_{ck}=0} = -\frac{G_{BVCCj'\_2} \cdot G_{BVCCj\_3} \cdot Z_{v\_bus}}{Z_{v\_busj'} \cdot Z_{v\_busj}}$$

1

.

(2)

$$\cdot \overline{1+T_m}$$

$$\left.\frac{\hat{y}_{ck}}{\hat{x}_{vj}}\right|_{\hat{x}_{vj'}=0,\hat{x}_{ck}=0} = \frac{G_{BCCCk\_2}\cdot G_{BVCCj\_3}\cdot Z_{v\_bus}}{Z_{v\_busj}}$$

(3)

$$\frac{1}{1+T_m}$$

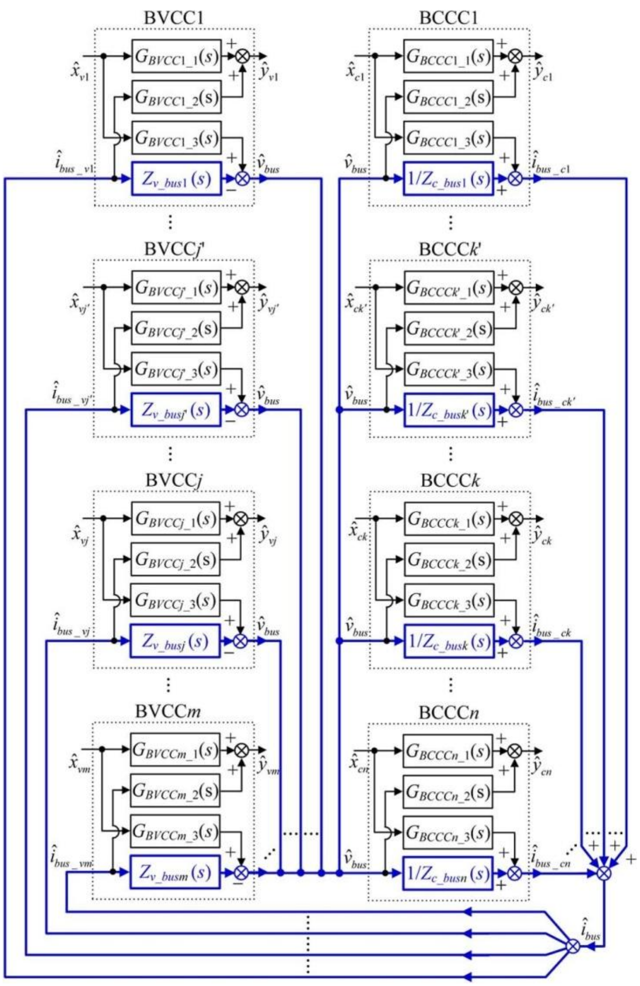

Fig. 5. Two-port small-signal model of the standard form of dc DPS.

TABLE II
DEFINITIONS OF VARIABLES AND INPUT-TO-OUTPUT TRANSFER FUNCTIONS OF TWO-PORT NETWORKS OF BVCCS AND BCCCS

	BVCC
x_{vj}	Input variable of the j^{th} BVCC at its non-bus side
y_{vj}	Output variable of the j^{th} BVCC at its non-bus side
G_{BVCCj_1}	x_{vj}-to-y_{vj} transfer function when the j^{th} BVCC works alone
G_{BVCCj_2}	i_{bus_vj}-to-y_{vj} transfer function when the j^{th} BVCC works alone
G_{BVCCj_3}	x_{vj}-to-v_{bus} transfer function when the j^{th} BVCC works alone
Z_{v_busj}	The j^{th} BVCC's bus-side port impedance when it works alone
	BCCC
x_{ck}	Input variable of the k^{th} BCCC at its non-bus side
y_{ck}	Output variable of the k^{th} BCCC at its non-bus side
G_{BCCCk_1}	x_{ck}-to-y_{ck} transfer function when the k^{th} BCCC works alone
G_{BCCCk_2}	v_{bus}-to-y_{ck} transfer function when the k^{th} BCCC works alone
G_{BCCCk_3}	x_{ck}-to-i_{bus_ck} transfer function when the k^{th} BCCC works alone
Z_{c_busk}	The k^{th} BCCC's bus-side port impedance when it works alone

(highlighted with thick arrows in Fig. 5). In order to facilitate this description, the expression of T_m is rearranged as follows:

$$T_m = \frac{Z_{v\_bus}}{Z_{c\_bus}} = \frac{\left(\sum_{j=1}^{m}\frac{1}{Z_{v\_busj}}\right)^{-1}}{\left(\sum_{k=1}^{n}\frac{1}{Z_{c\_busk}}\right)^{-1}} \quad (7)$$

$$\left.\frac{\hat{y}_{ck}}{\hat{x}_{ck}}\right|_{\hat{x}_{vj}=0,\hat{x}_{ck'}=0} = G_{BCCCk\_1} - \frac{G_{BCCCk\_2}G_{BCCCk\_3}Z_{v\_bus}}{1+T_m}$$

(4)

here Z_{v_bus} and Z_{c_bus} are the shunt impedance of the bus- side-port-impedances of all the BVCCs and BCCCs, respec- tively.

Finally, the proposed impedance-based stability criterion is given in the following two steps:

Step 1: Convert the target dc DPS into the standard form of dc DPS, and in the process classify all converters as BVCCs and BCCCs in the target dc DPS.

Step 2: Substitute the bus-side-port-impedances of BVCCs and BCCCs into (7), and verify whether T_m meets the Nyquist stability criterion. Specifically, if T_m satisfies the Nyquist criterion, then the system is stable.

$$\left.\frac{\hat{y}_{ck'}}{\hat{x}_{ck}}\right|_{\hat{x}_{vj}=0,\hat{x}_{ck'}=0} = -\frac{G_{BCCCk'\_2}\cdot G_{BCCCk\_3}\cdot Z_{v\_bus}}{1+T_m} \tag{5}$$

$$\left.\frac{\hat{y}_{vj}}{\hat{x}_{ck}}\right|_{\hat{x}_{vj}=0,\hat{x}_{ck'}=0} = \frac{G_{BVCCj\_2}\cdot G_{BCCCk\_3}\cdot Z_{v\_bus}}{Z_{v\_busj}} \cdot \frac{1}{1+T_m} \tag{6}$$

According to the Nyquist criterion, the basic stability requirement for the standard dc DPS is that there are no right-half-plane (RHP) poles in the input-to-output transfer functions (1) to (6). Furthermore, if the BVCCs and BCCCs are stable when operating independently, there will be no RHP poles in their own input-to-output transfer functions, i.e., , , , , , , and . Therefore, if there are no RHP poles in the expression of $1/(1+T_m)$, the system will be stable. In other words, T_m can be equivalently treated as the loop gain of the standard dc DPS

$G_{BCCCk\_1}(s)$ $G_{BVCCj\_1}(s)$ $G_{BVCCj\_3}(s)$ $Z_{v\_busj}(s)$ $G_{BCCCk\_1}(s)$ $G_{BCCCk\_2}(s)$ $G_{BCCCk\_3}(s)$ $Z_{c\_busk}(s)$

IV. EXTENSION AND APPLICATION OF THE PROPOSED IMPEDANCE-BASED STABILITY CRITERION

Although the original purpose of the proposed criterion is to evaluate the stability of some complex dc DPSs, such as PV-battery hybrid system, this impedance-based stability cri- terion is also applicable to other dc DPSs. In this section, the proposed criterion is applied to a standalone PV-battery hybrid system. Then, this criterion is extended to other dc DPS ap- plications, such as voltage-source systems, current-source sys- tems, dc DPSs whose source converters utilize the droop con- trol method and dc DPSs involving series-parallel connection of converters. It is shown that, compared with the existing sta- bility criteria, our approach does not only provide a convenient alternative analytical path, but also overcomes the limitation of the existing stability criteria.

A. Application to PV-Battery Hybrid System

First, according to the analysis in Section II, Fig. 6 shows the standard form of the standalone PV-battery hybrid system.

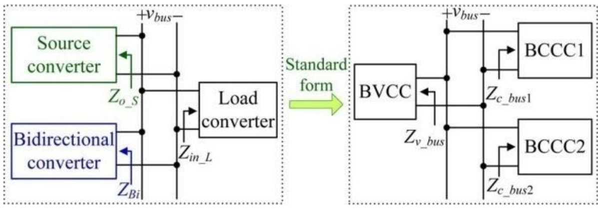

Fig. 6. Standard form of the standalone PV-battery hybrid system.

TABLE III
BVCCS AND BCCCS OF THE STANDALONE P
N
OPERATING MODES

	BVCC	BCCC1	BCCC2
Mode I	N/A*	N/A*	N/A*
Mode II	Bidirectional converter	Source converter	Load converter
Mode III	Bidirectional converter	Source converter	Load converter
Mode IV	Source converter	Bidirectional converter	Load converter
Mode V	Source converter	Bidirectional converter	Load converter
	Z_{v_bus}	Z_{c_bus1}	Z_{c_bus2}
Mode I	N/A*	N/A*	N/A*
Mode II	Z_{Bi}	Z_{o_S}	Z_{in_L}
Mode III	Z_{Bi}	Z_{o_S}	Z_{in_L}
Mode IV	Z_{o_S}	Z_{Bi}	Z_{in_L}
Mode V	Z_{o_S}	Z_{Bi}	Z_{in_L}

F ce system.

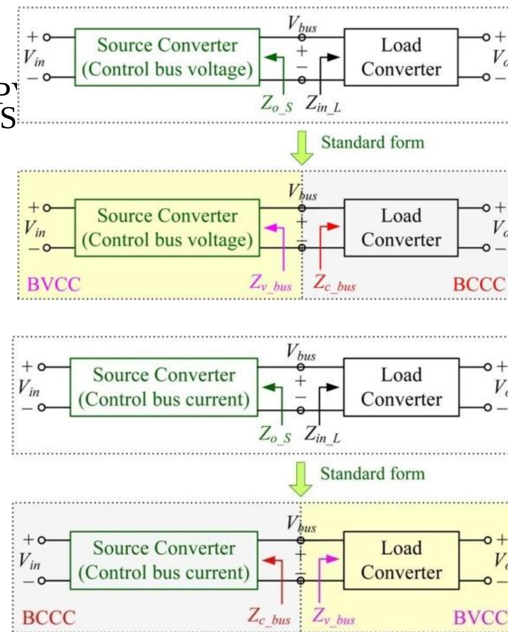

Fig. 8. Standard form of the current-source system.

In a likewise manner, using (7), the minor loop gain of thevoltage-source system can be expressed as

TABLE IV
MINOR LOOP GAINS OF THE STANDALONE PV-BATTERY HYBRID SYSTEM IN
OPERATING MODES I TO IV

$$T_m = \frac{Z_{v\_bus}}{Z_{c\_bus}} = \frac{Z_{o\_S}(s)}{Z_{in\_L}(s)}$$

C. Application to Current-Source System

ISSN: 2278-4632
Vol-10 Issue-3 No.01 March 2020

(8)

	Minor loop gain
Mode I	N/A*
Mode II	$T_m = \frac{Z_{v\_bus}}{Z_{c\_bus}} = \frac{Z_{Bi}(s)}{Z_{o\_S}(s) \parallel Z_{in\_L}(s)}$
Mode III	$T_m = \frac{Z_{v\_bus}}{Z_{c\_bus}} = \frac{Z_{Bi}(s)}{Z_{o\_S}(s) \parallel Z_{in\_L}(s)}$
Mode IV	$T_m = \frac{Z_{v\_bus}}{Z_{c\_bus}} = \frac{Z_{o\_S}(s)}{Z_{Bi}(s) \parallel Z_{in\_L}(s)}$
Mode V	$T_m = \frac{Z_{v\_bus}}{Z_{c\_bus}} = \frac{Z_{o\_S}(s)}{Z_{Bi}(s) \parallel Z_{in\_L}(s)}$

Since the source converter controls the bus current in a cur- rent-source system, the source converter acts as a BCCC. As the bus current is already regulated by the source converter, the load converter can only affect the bus voltage by changing its output power. Therefore, the load converter is a BVCC. Fig. 8 shows the standard form of the current-source system.

Again, using (7), we obtain the minor loop gain of the current- source system as

$$T_m = \frac{Z_{v\_bus}}{Z_{c\_bus}} = \frac{Z_{in\_L}(s)}{Z_{o\_S}(s)} \quad (9)$$

* In mode I, the PV-battery hybrid system is shut down, and it is stable.

Table III shows the BVCCs and BCCCs of the system in modesI to V.

Then, using (7), the minor loop gain of the standalone PV-bat- tery hybrid system in operating modes I to V can be found, as shown in Table IV. If all the converters are stable individually, and the minor loop gain in each mode satisfies the Nyquist cri- terion, the PV system will be stable in the corresponding mode.

B. Application to Voltage-Source System

Since the source converter controls the bus voltage in a voltage-source system, the source converter acts as a BVCC. Since the bus voltage is regulated by the source converter, the load converter can only affect the bus current by changing the load condition. Therefore, the load converter is a BCCC. Fig. 7shows the standard form of the voltage-source system.

D. Application to DC DPS With Source Converters Employing Droop Control

Fig. 9 gives a typical dc DPS whose source converters employ droop control. In this system, since source converters with precise control of the output voltage cannot be connected in parallel directly, the output voltage droop control is usually adopted [24]. Here, $Z_{o\_Sj}(s)(j = 1, 2, 3, \ldots, m)$ is the output impedance of the j-th source converter, and $Z_{in\_Lk}(s)(k = 1, 2, 3, \ldots, n)$ is the input impedance of the k-th load converter.

The proposed impedance-based stability criterion can be ap- plied to this system as follows. First, since the bus voltage is controlled by the source converters, and these source converters are working independently, each source converter can be treated as a BVCC. In addition, since the bus voltage is regulated by the source converters, the load converters can only affect the bus current by changing their output power. Hence, the load con- verters are BCCCs. Fig. 9 also shows the standard form of the

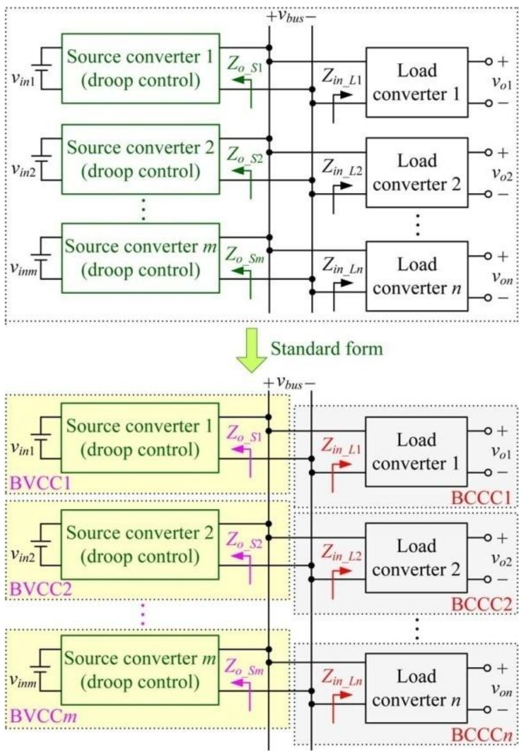

Fig. 9. Standard form of the dc DPS whose source converters are controlled by droop method.

dc DPS, in which droop control is utilized for the source con-verters.
Using (7), the minor loop gain of the dc DPS with source converters controlled by droop method can be expressed as

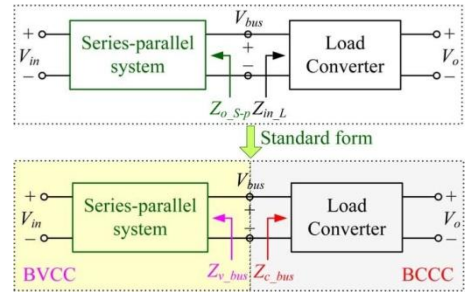

Fig. 10. Standard form of the dc DPS with source converter being a series- parallel connected system.

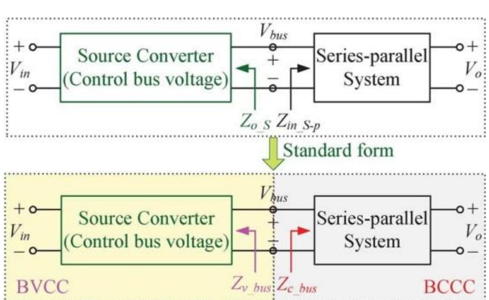

Fig. 11. Standard form of the dc DPS whose load converter is a series-parallel connected system.

bus voltage, the whole system can be treated as a BVCC. Since the bus voltage is already controlled by the series-parallel con- nected system, the load converter can only change the bus cur- rent by regulating its load condition. Hence, the load converter is a BCCC. Fig. 10 shows the standard form of this system.

Using (7), the minor loop gain of the dc DPS with the source converter being a series-parallel connected system can be ex- pressed as

$$T_m = \frac{Z_{v\_bus}}{Z_{c\_bus}} = \frac{\left(\sum_{j=1}^{m} \frac{1}{Z_{v\_busj}}\right)^{-1}}{\left(\sum_{k=1}^{n} \frac{1}{Z_{c\_busk}}\right)^{-1}} = \frac{\left(\sum_{j=1}^{m} \frac{1}{Z_{o\_Sj}}\right)^{-1}}{\left(\sum_{k=1}^{n} \frac{1}{Z_{in\_Lk}}\right)^{-1}} \quad (10)$$

Thus, according to the proposed criterion and (10), if all the converters are stable individually, and T_m satisfies the Nyquist criterion, the dc DPS is stable.

E. Application to DC DPS Containing Series-Parallel Connections

It is known that series-parallel connected systems are often employed in dc DPS to satisfy certain critical applications, e.g., high input voltage or current, high output voltage or current. Generally, there are four basic architectures of series-parallel connected systems: input-parallel output-parallel (IPOP), input-parallel output-series (IPOS), input-series output-parallel (ISOP), and input-series output-series (ISOS) systems. It is worth noting that in order to guarantee proper operation, appro- priate control strategies for sharing voltages or currents among the system's converters are indispensable [25].

Since the converters of a series-parallel connected system cannot work individually, the whole system can only be treated as a single converter. In other words, the series-parallel con- nected system is a complex converter controlling its output voltage.

Therefore, if the series-parallel connected system acts as a source converter, the dc DPS's stability can be assessed as fol- lows. Since the series-parallel connected system controls the

$$T_m = \frac{Z_{v\_bus}}{Z_{c\_bus}} = \frac{Z_{o\_S-p}(s)}{Z_{in\_L}(s)} \quad (11)$$

where $Z_{o\_S-p(s)}$ is the output impedance of the series-parallel connected system.

According to the proposed criterion and (11), if the series-par- allel connected system and the load converter are stable Individ- ually, and the minor loop gain satisfies the Nyquist criterion, the dc DPS is stable.

Similarly, if the series-parallel connected system acts as a load converter, the dc DPS's stability can be assessed as fol- lows. Since the series-parallel connected system's input voltage is usually controlled by the source converter, the source con- verter is a BVCC while the series-parallel connected system is a BCCC. Fig. 11 shows the standard form of this system.

Using (7), the minor loop gain of the dc DPS whose load con- verter employs a series-parallel connected system can be ex- pressed as:

$$T_m = \frac{Z_{v\_bus}}{Z_{c\_bus}} = \frac{Z_{o\_S}(s)}{Z_{in\_S-p}(s)} \quad (12)$$

where $Z_{in\_S-p(s)}$ is the input impedance of the series-parallel connected system.

According to the proposed criterion and (12), if the series-par- allel connected system and the load converter are stable individ- ually and the minor loop gain satisfies the Nyquist criterion, the dc DPS is stable.

From the above examples, we see that the proposed criterion is generally applicable to all kinds of dc DPSs.

ISSN: 2278-4632
Vol-10 Issue-3 No.01 March 2020

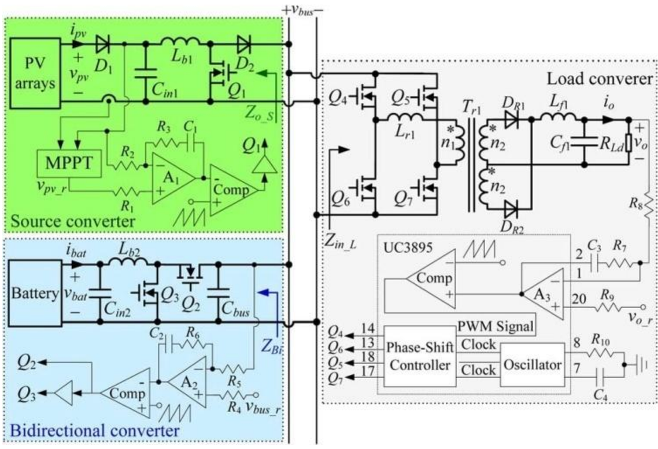

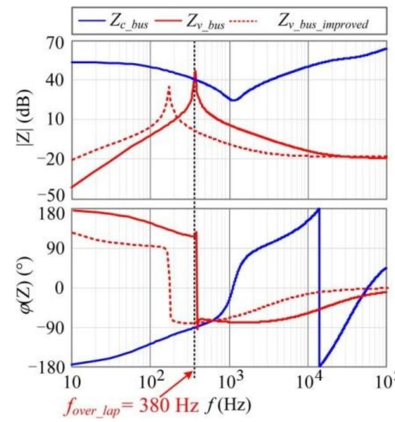

Fig. 12. Standalone PV-battery hybrid system.

TABLE V
MAIN CIRCUIT PARAMETERS OF THE STANDALONE PV-BATTERY HYBRID SYSTEM

Parameters	C_{in1}	C_{in2}	C_{bus}	C_{f1}	L_{b1}
Value	100 μF	220 μF	100 μF	680 μF	2 mH
Parameters	L_{b2}	L_{r1}	L_{f1}	T_{r1}	R_{Ld}
Value	2.5 mH	2 μH	250 μH	5:1	4.8 Ω

V. EXPERIMENTAL VERIFICATION

As discussed in the foregoing section, conventional stability criteria cannot readily assess the stability of the standalone PV-battery hybrid system operating in mode II. Application of the proposed criterion, however, conveniently resolves the problem. For verification, a 480 W standalone PV-battery hybrid system operating in mode II is constructed and tested in the Section V-A. Furthermore, application of the proposed criterion to other dc DPSs is verified with a 200 W experimental dc DPS whose source converter is controlled by droop method, as reported in Section V-B.

A. *Standalone PV-Battery Hybrid System*

Fig. 12 shows the PV-battery hybrid system. In this system, the source converter is a boost converter with MPPT control. The maximum output power of the PV arrays is 240 W and the output voltage of the PV arrays at the maximum power point is 250 V. The bidirectional converter is a buck-boost bidirectional converter, which regulates the bus voltage at 360 V. Here, the battery, whose output voltage is 220 V, can provide 240 W to the dc bus. The load converter is a phase-shifted full-bridge v_{bat} converter, whose output power and output voltage is 480 W and 48 V, respectively. Table V gives the parameters of the main circuit of the PV-battery hybrid system.

According to Table IV, the minor loop gain of the standalone PV-battery hybrid system can be expressed as:

$$T_m = \frac{Z_{v\_bus}}{Z_{c\_bus}} = \frac{Z_{Bi}(s)}{Z_{o\_S}(s)||Z_{in\_L}(s)} \qquad (13)$$

Using the small-signal circuit models of the source converter, the bidirectional converter and the load converter [26], Bodeplots of Z_{v_bus} and Z_{c_bus} at full load are given in solid lines shown in Fig. 13. From this figure, the intersection betweenand at about 380 Hz (f_{over_lap} in Fig. 13) is

$|Z_{v\_bus}|$ $|Z_{c\_bus}|$

ISSN: 2278-4632
Vol-10 Issue-3 No.01 March 2020

clearly evident. In addition, the difference between $\varphi(Z_{v\_bus})$ and $\varphi(Z_{c\_bus})$ is larger than 180° at about 380 Hz. Hence, the minor loop gain, Z_{v_bus}/Z_{c_bus}, will encircle $(-1, j0)$. In other

Fig. 13. Bode plots of Z_{v_bus} and Z_{c_bus} in PV-battery hybrid system at full load.

words, the PV-battery hybrid system will be unstable and oscil-late at about 380 Hz.

The experimental waveforms of the PV-battery hybrid system at full load are shown in Fig. 14. Fig. 14(a) shows the waveforms of i_o, v_o, i_{pv}, v_{pv}, i_{bat} and v_{bat}, where v_o, v_{pv}, v_{bat} and v_{bus} are their AC components. Oscillations in v_{bus}, i_{pv}, v_{pv}, i_{bat} and v_{bat} are observed, and the PV-battery system is unstable. In order to show the oscillations clearly, Fig. 14(b) shows the enlarged waveforms during the time period Δt of Fig. 14(a). It can be seen that the frequency of oscillation is about 380 Hz, which is consistent with the intersection frequency of $|Z_{v\_bus}|$ and $|Z_{c\_bus}|$ shown in Fig. 13. Since the oscillation of v_{bus} is suppressed effectively by the output voltage regulator of the load converter, there are no significant oscillations in i_o and v_o in Fig. 14. It is worth noting that, though the dc DPS is unstable, the system can only operate with an under-damped resonance instead of divergent resonance. This can be explained as follows. If the system is unstable, the current of converter's inductor starts to diverge. However, since all the converters are dc/dc converters, they operate in discontinuous current mode (DCM) when their inductor's current resonates to zero. Fortunately, in DCM, the converter's order will be reduced and the whole system could readily return to stable operation. As a result, the current ceases to diverge and converges again. Finally, the system reaches an equilibrium state, and behaves as under-damped resonance [27].

According to the proposed criterion, a total separation between $|Z_{v\_bus}|$ and $|Z_{c\_bus}|$ can ensure the stability of the experimental PV-battery system. It is well known that there are many existing solutions to reduce Z_{v_bus}'s amplitude in order to realize this target [28]–[31]. However, as our focus in this paper is to assess the stability of dc DPS rather than to adjust the converter's impedance, we only utilize the most practical and simplest way to reduce $|Z_{v\_bus}|$, i.e., increasing C_{bus} [28]. According to the proposed criterion, we change the PV-battery hybrid system's C_{bus} from 100 μF to 470 μF. As a result, the amplitude of the improved Z_{v_bus} is lower than the amplitude of Z_{c_bus} in the whole frequency range and the improved PV-bat- tery system should be stable. Fig. 13 also shows the improved Bode plots of Z_{v_bus} in dash lines.

The experimental waveforms of the improved PV-battery system at full load are shown in Fig. 15. Fig. 15(a) shows the waveforms of i_o, v_o, i_{pv}, v_{pv}, i_{bat}, and v_{bat}, where v_o, i_{pv}, v_{pv}, i_{bat}, and v_{bus} are their AC components. Furthermore, Fig. 15(b) shows the enlarged waveforms during the time period of Fig. 15(a). It can be seen that oscillations in the

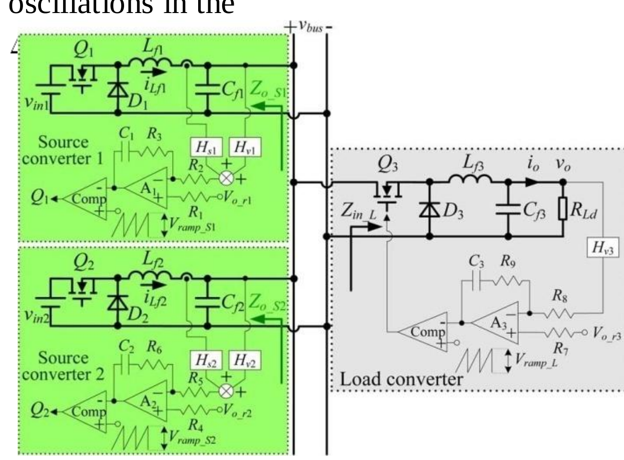

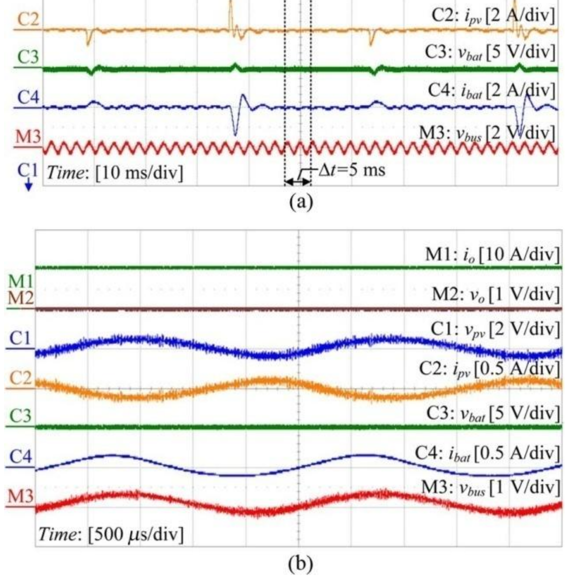

Fig. 14. Experimental waveforms of standalone PV-battery hybrid system at full load. (a) Waveforms of voltage and current. (b) Enlarged waveforms of voltage and current during the time

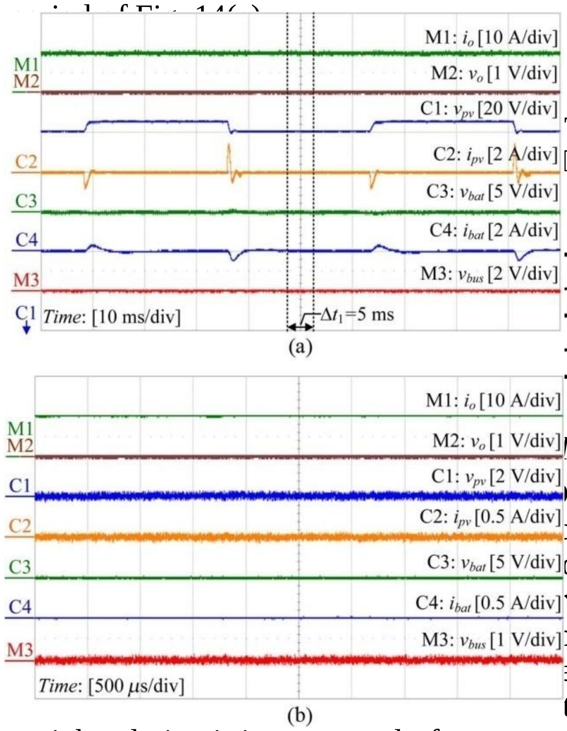

are controlled by droop control.

TABLE VI
THE DC DPS WHOSE SOURCE CONVERTERS
DROOP CONTROL

C_{f2}
100 μF
R_{Ld}
0.72 Ω

lled by Droop Method

PS, in which droop control is applied to the source converter 2 are the same buck converters operating at a ource converter's input voltage, output voltage and espectively. In addition, the source converter employs factor is

erter operating at a switching frequency of 100 kHz. Its tage is regulated at 12 V by the PI regulator whose peripheral circuit is composed of R_7 , R_8 , R_9 and C_3. Table VI gives the parameters of the main circuit of the dc DPS whose source converters are controlled by droop method.

Using (10), the equivalent loop gain of the above dc DPS with source converters controlled by droop method can be expressed as:

Fig. 15. Experimental waveforms of the improved PV-battery system at full load. (a) Waveforms

ISSN: 2278-4632
Vol-10 Issue-3 No.01 March 2020

of voltage and current. (b) Enlarged waveforms of voltage and current during the time period Δt_1 of Fig. 15(a).

voltages and currents in the PV-battery system have ceased. Therefore, the improved system is stable, which is consistent with Fig. 13.

In summary, the experimental results given in Figs. 14 and 15 showed that the proposed impedance-based stability criterion can evaluate the stability of the PV-battery hybrid system in mode II effectively.

$$T_m = \frac{Z_{v\_bus}}{Z_{c\_bus}} = \frac{(Z_{o\_S1}(s) \| Z_{o\_S2}(s))}{Z_{in\_L}(s)} \quad (14)$$

According to the small-signal circuit model of the source con- verter [24] and the load converter [26], the Bode plots of Z_{v_bus} and Z_{c_bus} at full load are presented in solid lines in Fig. 17. It can be seen that there are intersections between $|Z_{v\_bus}|$ and $|Z_{c\_bus}|$ at about 1.54 kHz and 1.9 kHz. Moreover, the differ- ence between $\varphi(Z_{v\_bus})$ and $\varphi(Zc\_bus)$ is larger than 180 $^\circ$ at 1.54 kHz. Hence, from the proposed criterion, the above dc DPS is unstable and oscillates at about 1.54 kHz.

The experimental waveforms of the above dc DPS with its source converter controlled by droop method at full load are shown in Fig. 18(a). The waveforms of i_o, i_{Lf1}, i_{Lf2}, v_{bus} and v_o are shown in particular. Here, i_{Lf1}, i_{Lf2}, v_{bus}, and v_o are their AC components. Oscillations are observed in i_o, i_{Lf1}, i_{Lf2}, v_{bus}, and v_o, and the frequency of oscillations is about 1.54 kHz.

This phenomenon is consistent with the Bode plots shown in Fig. 17 where the difference between $\varphi(Z_{v\_bus})$ and $\varphi(Z_{c\_bus})$

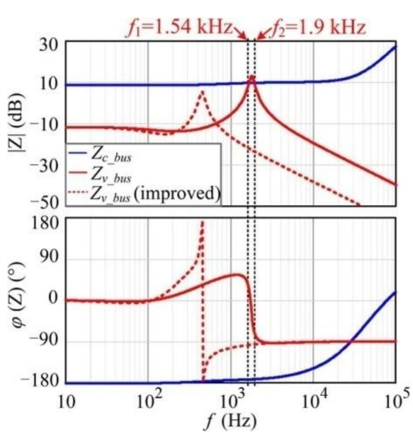

Fig. 17. Bode plots of Z_{v_bus} and Z_{c_bus} in dc DPS whose source converters employ droop control at full load.

ISSN: 2278-4632
Vol-10 Issue-3 No.01 March 2020

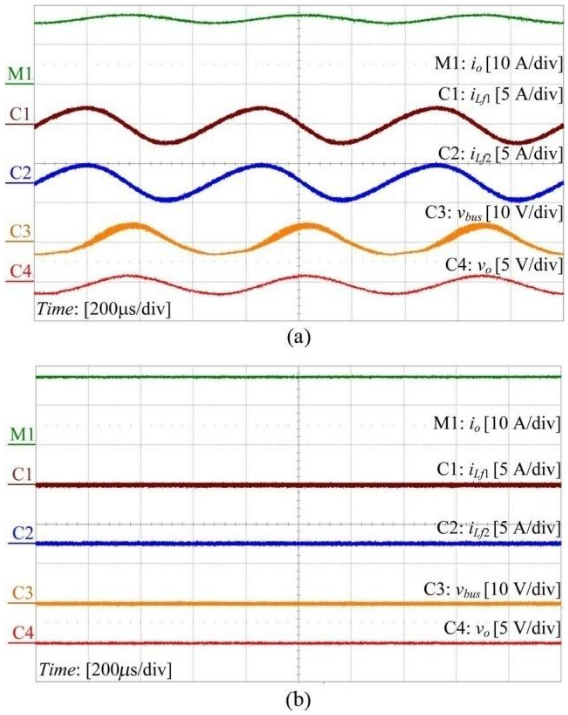

Fig. 18. Experimental waveforms of the improved dc DPS whose source con- verter employs droop control at full load. (a) Original system. (b) Improved system.

is larger than 180° at the amplitude interaction frequency 1.54 kHz.

It is known that decreasing the amplitude of Z_{o_bus} can avoid undesirable intersection between $|Z_{bus}|$ and $|Z_{o\_bus}|$ to en- sure system's stability. Hence, considering the amplitude of the buck converter's output impedance being inversely proportional to its output filter capacitor [32], we modify the parameters of the above dc DPS. Specifically, the values of C_{f1} and C_{f2} are changed from 100 μF to 680 μF. Fig. 17 also shows the im- proved Bode plots of Z_{o_bus} in dash lines. It can be seen that intersection between $|Z_{in\_bus}|$ and $|Z_{o\_bus}|$ has ceased. There- fore, the improved dc DPS with its source converter controlled by droop method should be stable.

The experimental waveforms of the improved dc DPS with its source converter controlled by droop method at full load are given in Fig. 18(b), where the waveforms of i_o, i_{Lf1}, i_{Lf2}, v_{bus} and v_o are shown. Here, i_{Lf1}, i_{Lf2}, v_{bus} and v_o are their AC components. No oscillations are observed in the voltages and currents in the improved dc DPS after increasing the values of C_{f1} and C_{f2}. Therefore, the improved dc DPS is stable, which is also consistent with the Bode plots shown in Fig. 17.

In summary, the experimental result given in Fig. 18 shows that the proposed impedance-based stability criterion can effec- tively predict instability of the dc DPS whose source converter is controlled by the droop method.

VI. CONCLUSIONS

The stability assessment of dc distributed power systems is discussed in this paper. A simple and generally applicable impedance-based stability criterion is proposed for assessing stability of dc distributed power systems. Our study shows that the proposed criterion is applicable to general dc DPSs, including the voltage-source system, current-source system, dc DPS with source converters employing droop control and dc DPS containing series-parallel connected system. Thus, compared with the existing stability criterion, our approach provides a convenient alternative analytical path to produce correct stability assessment, and overcomes the limitation of the existing stability criteria.

REFERENCES

[1] C. D. Xu and K. W. E. Cheng, "A survey of distributed power system-AC versus DC distributed power system," in *Proc. IEEE PESA*, 2011, pp. 1–12.

[2] F. Blaabjerg, A. Consoli, J. A. Ferreira, and J. D. van Wyk, "The future of electronic power processing and conversion," *IEEE Trans. Power Electron.*, vol. 20, no. 3, pp. 715–720, 2005.

[3] A. L. Julian and R. M. Cuzner, "Design, modeling and stability analysis of an integrated shipboard DC power system," in *Proc. IEEE ESTS*, 2009, pp. 428–432.

[4] A. Emadi, A. Khaligh, C. H. Rivetta, and G. A. Williamson, "Con- stant power loads and negative impedance instability in automotive systems: Definition, modeling, stability, control of power electronic converters and motor drives," *IEEE Trans. Veh. Technol.*, vol. 55, no. 4, pp. 1112–1124, 2006.

[5] Y. Liu, A. Pratt, P. Kumar, M. Xu, and F. C. Lee, "390 V Input VRM for High Efficiency Server Power Architecture," in *Proc. IEEE APEC*, 2007, pp. 1619–1624.

[6] A. Pratt, P. Kumar, and T. V. Aldridge, "Evaluation of 400 V DC distri- bution in telco and datacenters to improve energy efficiency," in *Proc. IEEE INTELEC*, 2007, pp. 32–39.

[7] D. Boroyevich, I. Cvetković, D. Dong, R. Burgos, F. Wang, and F. C. Lee, "Future electronic power distribution systems—A contemplative view," in *Proc. IEEE Optim. Electr. Electron. Equip. Int. Conf.*, 2010, pp. 1369–1380.

[8] X. Feng, J. Liu, and F. C. Lee, "Impedance specifications for stable DC distributed power systems," *IEEE Trans. Power Electron.*, vol. 17, no. 2, pp. 157–162, 2002.

[9] A. Emadi, "Modeling of power electronic loads in AC distribution sys- tems using the generalized state-space averaging method," *IEEE Trans. Ind. Electron.*, vol. 51, no. 5, pp. 995–1000, 2004.

[10] X. L. Xiong, C. K. Tse, and X. B. Ruan, "Bifurcation analysis of stand- alone photovoltaic-battery hybrid power system," *IEEE Trans. Circuits Syst. I, Reg. Papers*, vol. 60, no. 5, pp. 1354–1365, 2013.

[11] A. Khaligh, "Realization of parasitics in stability of DC-DC con- verters loaded by constant power loads in advanced multi-converter automotive systems," *IEEE Trans. Ind. Electron.*, vol. 55, no. 6, pp. 2295–2305, 2008.

[12] M. Huang, C. K. Tse, S. C. Wong, C. Wan, and X. B. Ruan, "Low- frequency hopf bifurcation and Its effects on stability margin in three-phase PFC power supplies connected to non-ideal power grid," *IEEE Trans. Circuits Syst. I, Reg. Papers*, vol. 60, no. 12, pp. 3328–3340, 2013.

[13] A. M. Rahimi and A. Emadi, "Active damping in DC/DC power electronic converters: A novel method to overcome the problems of constant power loads," *IEEE Trans. Ind. Electron.*, vol. 56, no. 5, pp. 1428–1439, 2009.

[14] M. Huang, S. C. Wong, C. K. Tse, and X. B. Ruan, "Catastrophic bifur- cation in three-phase voltage-source converters," *IEEE Trans. Circuits Syst. I, Reg. Papers*, vol. 60, no. 4, pp. 1062–1071, 2013.

ISSN: 2278-4632
Vol-10 Issue-3 No.01 March 2020

[15] R. D. Middlebrook, “Input filter considerations in design and applica- tion of switching regulators,” in *Proc. IEEE IAS*, 1976, pp. 366–382.
[16] C. M. Wildrick, F. C. Lee, B. H. Cho, and B. Choi, “A method of defining the load impedance specification for a stable distributed power system,” *IEEE Trans. Power Electron.*, vol. 10, no. 3, pp. 280–285, 1995.
[17] H. Phuong and B. H. Cho, “A new methodology for the stability anal- ysis of large-scale power electronics systems,” *IEEE Trans. Circuits Syst. I, Fundam. Theory Appl.*, vol. 45, no. 4, pp. 377–385, 1998.
[18] H. H. C. Iu and C. K. Tse, “Study of low-frequency bifurcation phe- nomena of a parallel-connected boost converter system via simple av- eraged models,” *IEEE Trans. Circuits Syst. I, Fundam. Theory Appl.*, vol. 50, no. 5, pp. 679–685, 2003.
[19] X. Zhang, X. B. Ruan, H. Kim, and C. K. Tse, “Adaptive active ca- pacitor converter for improving stability of cascaded DC power supply system,” *IEEE Trans. Power Electron.*, vol. 28, no. 4, pp. 1807–1816, 2013.
[20] J. Calvente, L. Martinez-Salamero, P. Garcés, and A. Romero, “Zero dynamics-based design of damping networks for switching converters,” *IEEE Trans. Aerosp. Electron. Syst.*, vol. 39, no. 4, pp. 1292–1303, 2003.
[21] J. Sun, “Impedance-based stability criterion for grid-connected in- verters,” *IEEE Power Electron. Lett.*, vol. 26, no. 11, pp. 3075–3078, 2011.
[22] B. Indu Rani, G. Saravana Ilango, and C. Nagamani, “Control strategy for power flow management in a PV system supplying DC loads,” *IEEE Trans. Power Electron.*, vol. 60, no. 8, pp. 3185–3194, 2013.
[23] L. Arnedo, “System level black-box models for DC-DC converters,” Ph.D. dissertation, Virginia Polytech. Inst. State Univ., Blacksburg, VA, USA, Sep. 2008.
[24] S. G. Luo, Z. Ye, R. L. Lin, and F. C. Lee, “A classification and evalua- tion of paralleling methods for power supply modules,” in *Proc. IEEE PESC*, 1999, pp. 901–908.
[25] W. Chen, X. Ruan, H. Yan, and C. K. Tse, “DC/DC conversion sys- tems consisting of multiple converter modules: Stability, control and experimental verifications,” *IEEE Trans. Power Electron.*, vol. 24, no. 6, pp. 1463–1474, 2009.
[26] S. Cuk, “Modeling, analysis, design of switching converters,” Ph.D. dissertation, California Inst. Technol., Pasadena, CA, USA, Nov. 1976.
[27] C. M. Wildrick, “Stability of distributed power supply system,” Ph.D. dissertation, Virginia Polytech. Inst. State Univ., Blacksburg, VA, USA, Feb. 1993.
[28] S. Abe, M. Hirokawa, T. Zaitsu, and T. Ninomiya, “Optimal bus ca- pacitance design for system stability in onboard distributed power ar- chitecture,” in *Proc. EPE-PEMC*, 2008, pp. 393–399.
[29] X. Liu, A. J. Forsyth, and A. M. Cross, “Negative input-resistance com- pensator for a constant power load,” *IEEE Trans. Ind. Electron.*, vol. 54, no. 6, pp. 3188–3196, 2007.
[30] A. M. Rahimi and A. Emadi, “Active damping in DC/DC power electronic converters: A novel method to overcome the problems of constant power loads,” *IEEE Trans. Ind. Electron.*, vol. 56, no. 5, pp. 1428–1439, 2009.
[31] M. Cespedes, L. Xing, and J. Sun, “Constant-power load system stabi- lization by passive damping,” *IEEE Power Electron. Lett.*, vol. 26, no. 7, pp. 1832–1836, 2011.
[32] T. Wu and X. Ruan, “Characterization of input/output impedance spec- ifications for DC distributed power system,” in *Proc. IEEE ISIE*, 2006, pp. 982–987.